XXXVI Ibero-Latin American Congress on Computational Methods in Engineering
CILAMCE
Rio de Janeiro, 22-25 Nov 2015

# VIBRATION-BASED DAMAGE IDENTIFICATION IN THIN-WALLED BEAMS WITH DIFFUSED CRACKING

**Patricia N. Dominguez**[1,3]

**Víctor H. Cortínez**[1,2,3]

vcortine@frbb.utn.edu.ar

pdoming@uns.edu.ar

1. Centro de Investigaciones en Mecánica Teórica y Aplicada, UTN-FRBB
   11 de abril 461, (8000) Bahía Blanca, Argentina.
2. Consejo de Investigaciones Científicas y Técnicas CONICET
3. Departamento de Ingeniería, Universidad Nacional del Sur
   Av. Alem 1253, (8000) Bahía Blanca, Argentina.

***Abstract.***

*This work deals with the identification of diffused damage in thin-walled beams. It is based on the development of a structural model for the dynamics of damaged thin-walled beams.*

*The identification problem consists in obtaining the damage parameters that minimize an objective function given by the quadratic relative difference between theoretical and experimental values of displacements (and/or natural frequencies). The optimization problem is solved by means of the Finite Element Method to evaluate the objective function and the Simulated Annealing technique to direct the search of the optimal parameters (location, length and depth) of cracks.*

*The methodology is shown to be efficient for identifying diffuse damage even in the case of existing measurement errors.*

***Keywords:*** *damaged thin-walled beams, diffused cracking, vibration based identification.*

## INTRODUCTION

Early crack detection in engineering structures is a fundamental task in order to avoid the possibility of catastrophic failures. Accordingly, the development of structural health monitoring techniques has acquired a remarkable importance.

In the last years, vibration-based techniques for damage identification have emerged as an attractive alternative to local inspection. They are based on the fact that damage induces a change in structural stiffness distribution, thus modifying the dynamic response. Accordingly, by measuring vibration of the damaged structure under known loadings, it is possible to estimate the location and magnitude of the damage with the help of mathematical models as interpretive tools.

These techniques were extensively studied in relation to slender structures. For these ones, a beam model captures the most significant features of the structural dynamics.

Most studies have focused on bending vibrations of Bernoulli-Euler and/or Timoshenko bi-symmetric solid section beams. On the other hand, non symmetric beams, such as thin-walled section beams, have not been addressed in depth, perhaps due to their more complex dynamics presenting bending, twisting and axial vibrations in a coupled form (Cortínez & Piovan, 2002). Recently, some studies were directed to fatigue crack detection methods for metallic thin-walled beams (Cortínez & Dominguez, 2014; Cortínez & Dotti, 2013; Cortínez et al., 2014; Dotti et al., 2015)

Many studies analyzing damage detection in beams were concerned on concentrated cracks, such as fatigue cracks in metallic structures.

However, there exist situations where damage has the form of diffuse cracking, as in the case of reinforced concrete beams. Some studies were directed to the identification of continuously cracked beams with solid cross-sections under flexural vibrations (Casas & Aparicio, 1994; Cerri & Vestroni, 2000, 2003; Hammed & Frostig, 2004; Razak & Choi, 2001; Zhu & Law, 2007).

One of the interesting aspects analyzed corresponds to the features of the related inverse problem for identifying damage from dynamic measures. For example, Cerri & Vestroni (2000) studied the damage identification in reinforced concrete beams using measured frequency changes. In that paper, a simple model of damage was assumed in which the zone affected by cracking is represented by a beam element with a bending stiffness $EI^D$ smaller than the undamaged value $EI^U$.

According to the authors' knowledge, no work was performed related to diffused cracking detection in thin-walled (or thick-walled) beams presenting coupled vibration motions.

In other to fill this gap, the present study deals with the identification of diffused damage in thin-walled (or thick-walled) beams from the knowledge of their dynamic response. For this purpose a theoretical model of the three dimensional dynamics of a thin- or thick-walled damaged beams is developed. Following Cerri & Vestroni (2000), damage is assumed to be given in the form of a change in the values of the stiffnesses in the zone affected by cracking.

The problem consists in obtaining the damage parameters that minimize an objective function given by the quadratic relative difference between theoretical and experimental displacement values (and/or frequency values). The optimization is approached by means of the Finite Element Method (MEF) to evaluate the objective function and the Simulated

Annealing technique (SA) to direct the search of the optimal parameters (location, length and depth) of the cracked zone.

The methodology is shown to be efficient for identifying diffuse damage even in the case of existing measurement errors.

# 1 STRUCTURAL MODEL OF A BEAM WITH DIFFUSE DAMAGE

In this section, the equations governing the dynamics of the structural system shown in "Fig. 1" are presented. It is considered a non-homogeneous cross-section with an arbitrary shape (it is possible to analyze thin- or thick-walled sections) and composed of several materials. Considering the fact that the damaged zone is characterized by a different shape with respect to the intact cross-section, it is not possible to employ a global system of reference with principal axes. Accordingly, the theoretical model is developed using arbitrary reference axes.

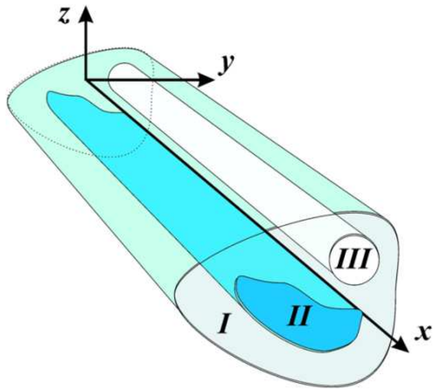


**Figure 1.Analyzed Structural Element**

The present theoretical model corresponds to the mechanics of a non-homogeneous beam and is used in an approximate form for considering a reinforced concrete beam with diffuse cracking.

## 1.1 Equations of motion

This theoretical model is based on the following assumption for the displacements field:

$$u_x = u(x,t) - \theta_z(x,t)y - \theta_y(x,t)z + \theta(x,t)\varphi(y,z)$$

$$u_y = v(x,t) - z\phi(x,t) \qquad (1)$$

$$u_z = w(x,t) + y\phi(x,t)$$

where $u_x$ represents the axial displacement in x- longitudinal direction, $u_y$ and $u_z$ transverse displacements, in y- and z-directions respectively, $u$, $v$ and $w$ constitute translational displacements of the cross-section, $\phi$ corresponds to twisting rotation, $\theta_y$ and $\theta_z$ are bending rotations, $\theta$ is a measure of the intensity of warping along the beam, and $\varphi$ is the Saint-Venant torsional warping function defined as the solution of the following problem:

$$\frac{\partial}{\partial y}\left(G\frac{\partial\varphi}{\partial y}\right)+\frac{\partial}{\partial z}\left(G\frac{\partial\varphi}{\partial z}\right)=0 \qquad y,z\in\Omega$$
$$\frac{\partial\varphi}{\partial n}=zl-ym \qquad y,z\in\Gamma \tag{2}$$

where $\Omega$ is the domain corresponding to the considered cross-section, $\Gamma$ is the boundary of this domain, $l=\cos(n,y)$, $m=\cos(n,z)$, with *n* denoting the unit vector normal to $\Gamma$, and $G$ is the transverse elasticity modulus.

The kinematic hypothesis (1) constitutes a generalization of that proposed by Cortínez & Piovan (2002) and is applicable to arbitrary cross-sectional shapes (including both cases, thin-walled or thick-walled sections).

From the displacement expressions (1), the following non-zero components of the strain tensor may be obtained as:

$$\varepsilon_x = u'-\theta_z' y-\theta_y' z+\theta'\varphi$$
$$\gamma_{xy}=\left(v'-\theta_z\right)-z\phi'+\theta\varphi_y \tag{3}$$
$$\gamma_{xz}=\left(w'-\theta_y\right)+y\phi'+\theta\varphi_z$$

with the following notation $(\cdot)'=\partial(\cdot)/\partial x$.

Assuming an elastic material, the stresses are obtained by using the Hooke's Law:

$$\sigma_x=E\varepsilon_x \qquad \tau_{xy}=G\gamma_{xy} \qquad \tau_{xz}=G\gamma_{xz} \tag{4}$$

The Young modulus *E*, the transverse elasticity modulus *G* and the density $\rho$ are supposed to vary with respect to *y* and *z*, making it possible to consider non-homogeneous cross-sections.

The dynamics of the analyzed structural system may be formulated by means of the Virtual Work Principle, including inertial forces:

$$\int_V\left(\sigma_x\delta\varepsilon_x+\tau_{xy}\delta\gamma_{xy}+\tau_{xz}\delta\gamma_{xz}\right)dV-\sum_{i=x,y,z}\left(\int_V(f_i-\rho\ddot{u}_i)\delta u_i dV+\int_S p_i\delta u_i dS\right)=0 \tag{5}$$

being $f_i$ and $p_i$ are volume and surface forces, respectively. In (5) a dot over the variables denotes derivatives with respect to time.

Substituting expressions (1), (3) and (4) into (5) and applying variational calculus, it is possible to arrive to the following equations of motion in terms of the beam stress resultants:

$$
\begin{aligned}
&-\frac{\partial N}{\partial x}+\rho_0\left(\ddot{u}A-\ddot{\theta}_z S_z-\ddot{\theta}_y S_y+\ddot{\theta}S_\varphi\right)=q_x \\
&\frac{\partial M_z}{\partial x}-Q_y+\rho_0\left(-\ddot{u}S_z+\ddot{\theta}_z I_z+\ddot{\theta}_y I_{yz}-\ddot{\theta}I_{\varphi y}\right)=-m_z \\
&\frac{\partial M_y}{\partial x}-Q_z+\rho_0\left(-\ddot{u}S_y+\ddot{\theta}_z I_{yz}+\ddot{\theta}_y I_y-\ddot{\theta}I_{\varphi z}\right)=-m_y \\
&-\frac{\partial Q_y}{\partial x}+\rho_0\left(\ddot{v}A-\ddot{\phi}S_y\right)=q_y \\
&-\frac{\partial Q_z}{\partial x}+\rho_0\left(\ddot{w}A+\ddot{\phi}S_z\right)=q_z \\
&-\frac{\partial B}{\partial x}-T_W+\rho_0\left(\ddot{u}S_\varphi-\ddot{\theta}_z I_{\varphi y}-\ddot{\theta}_y I_{\varphi z}+\ddot{\theta}C_W\right)=b \\
&-\frac{\partial (T_{SV}+T_W)}{\partial x}+\rho_0\left(-\ddot{v}S_y+\ddot{\phi}I_y+\ddot{w}S_z+\ddot{\phi}I_z\right)=m_x
\end{aligned}
\tag{6}
$$

Along with the following end conditions:

$$
\begin{aligned}
&N=\tilde{N} && \delta u=0 \\
&M_z=\tilde{M}_z && \delta\theta_z=0 \\
&M_y=\tilde{M}_y && \delta\theta_y=0 \\
&Q_z=\tilde{Q}_z && \delta w=0 \\
&Q_y=\tilde{Q}_y && \delta v=0 \\
&B=\tilde{B} && \delta\theta=0 \\
&T_{SV}+T_W=\tilde{M}_T && \delta\phi=0
\end{aligned}
\tag{7}
$$

In the above expressions, $q_x(x,t),\ q_y(x,t),\ q_z(x,t)$ are distributed forces per unit length, $m_x(x,t),\ m_y(x,t),\ m_z(x,t)$ are external moments per unit length and $b$ is the external bimoment per unit length. These forces include viscous damping. $\rho_0$ corresponds to the density of a reference material considering the fact that the cross section may be non-homogeneous. $\tilde{N},\tilde{M}_y,\tilde{M}_z,\tilde{Q}_y,\tilde{Q}_z,\tilde{B}$ and $\tilde{M}_T$ are external sectional stress resultants applied at the ends of the beam.

The beam stress resultants are defined in the following form:

$$
\begin{aligned}
&N = \overline{EA}u' - \overline{ES_z}\theta_z' - \overline{ES_y}\theta_y' + \overline{ES_\varphi}\theta' \\
&M_y = \overline{ES_y}u' - \overline{EI_{yz}}\theta_z' - \overline{EI_y}\theta_y' + \overline{EI_{\varphi z}}\theta' \\
&M_z = \overline{ES_z}u' - \overline{EI_z}\theta_z' - \overline{EI_{yz}}\theta_y' + \overline{EI_{\varphi y}}\theta' \\
&B = \overline{ES_\varphi}u' - \overline{EI_{\varphi y}}\theta_z' - \overline{EI_{\varphi z}}\theta_y' + \overline{EC_W}\theta' \\
&Q_y = \overline{GA}\left(v' - \theta_z\right) - \overline{GS_y}\left(\phi' - \theta\right) \\
&Q_z = \overline{GA}\left(w' - \theta_y\right) + \overline{GS_z}\left(\phi' - \theta\right) \\
&M_T = T_{SV} + T_W \\
&T_{SV} = \overline{GJ}\phi' \\
&T_W = \overline{GS_z}\left(w' - \theta_y\right) - \overline{GS_y}\left(v' - \theta_z\right) + \overline{GD}\left(\phi' - \theta\right)
\end{aligned}
\tag{8}
$$

The sectional stiffness coefficients are determined as:

$$
\begin{aligned}
&A = \int_A \frac{\rho}{\rho_0} dA, \quad S_z = \int_A \frac{\rho}{\rho_0} y dA, \quad S_y = \int_A \frac{\rho}{\rho_0} z dA, \quad S_\varphi = \int_A \frac{\rho}{\rho_0} \varphi dA, \quad C_W = \int_A \frac{\rho}{\rho_0} \varphi^2 dA \\
&I_z = \int_A \frac{\rho}{\rho_0} y^2 dA, \quad I_y = \int_A \frac{\rho}{\rho_0} z^2 dA, \quad I_{yz} = \int_A \frac{\rho}{\rho_0} yz dA, \quad I_{\varphi z} = \int_A \frac{\rho}{\rho_0} \varphi z dA, \quad I_{\varphi y} = \int_A \frac{\rho}{\rho_0} \varphi y dA \\
&D = \int_A \frac{\rho}{\rho_0}\left(\varphi_y^2 + \varphi_z^2\right) dA, \quad J = \int_A \frac{\rho}{\rho_0}\left(y^2 + z^2\right) dA - D \\
&\overline{EA} = \int_A E dA, \quad \overline{ES_z} = \int_A E y dA, \quad \overline{ES_y} = \int_A E z dA, \quad \overline{ES_\varphi} = \int_A E \varphi dA, \quad \overline{EC_W} = \int_A E \varphi^2 dA, \\
&\overline{EI_z} = \int_A E y^2 dA, \quad \overline{EI_y} = \int_A E z^2 dA, \quad \overline{EI_{yz}} = \int_A E yz dA, \quad \overline{EI_{\varphi y}} = \int_A E \varphi y dA, \quad \overline{EI_{\varphi z}} = \int_A E \varphi z dA, \\
&\overline{GA} = \int_A G dA, \quad \overline{GS_y} = \int_A G z dA, \quad \overline{GS_z} = \int_A G y dA, \quad \overline{GD} = \int_A G\left(\varphi_y^2 + \varphi_z^2\right) dA, \quad \overline{GJ} = \int_A G\left(y^2 + z^2\right) dA - D
\end{aligned}
\tag{9}
$$

It should be observed that the present model takes into account shear deformation effects and rotary and warping inertias, and may be considered as an extension of the Timoshenko´s theory for three dimensional motion of beams (Cortínez & Piovan, 2002).

## 1.2 Diffuse cracking model

Distribution of cracking in the damaged zone of the beam depends on the causes of damage and, in general, is not uniform. However, in a simplified form and following the approach proposed by Cerri & Vestroni (2002), damage is described by means of three parameters: the coordinate indicating the start of the cracked zone $x_f$, the length of the zone

$l_f$ and the depth of the cracks $a_f$. In this paper, the last one is assumed to be constant for the damaged zone. As an example this paper deals with a double T section in which one of the webs is damaged ("Fig. 2").

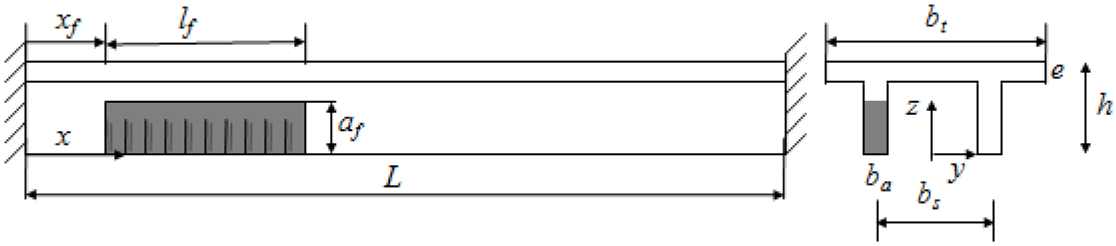


**Figure 2. Damaged beam under study**

Of course, it is possible to consider more complex types of damages. However, the present simplified form is interesting to study the salient features of the identification problem. It is assumed that once produced, the cracks do not close during vibrations of small amplitude. There is experimental evidence demonstrating this fact for reinforced concrete beams, differently to the case of metallic beams with fatigue cracks.

## 2 DAMAGE IDENTIFICATION PROBLEM

Identification based on the modification in dynamic response may be carried out by minimizing the difference, using an appropriate norm, between measured response magnitudes and those theoretically calculated with the present model. Such an estimation is performed for different feasible values of $x_f$, $a_f$ and $l_f$ that define the damaged zone.

In this work, two alternatives for identification are considered. One of them is based on the measurement of natural frequencies and the other one on the measurement of forced displacements under known applied loadings. In the following subsections these identification problems are formulated.

### 2.1 Identification by means of natural frequencies

Adopting a minimum squares criteria, the damage identification problem may be formulated as one of optimization in the following form:

$$\left\{a_f, x_f, l_f\right\} = \arg\min(FO) \tag{10}$$

where

$$FO = \sum_{n=1}^{N} \left( \frac{\tilde{\omega}_n - \omega_n}{\tilde{\omega}_n} \right)^2 \tag{11}$$

s.t.

$$0 \le x_f \le x_f^{max}$$
$$a_f^{min} \le a_f \le a_f^{max} \qquad (12)$$
$$l_f^{min} \le l_f \le l_f^{max}$$

being $\tilde{\omega}_n$ the *n-th* measured natural frequency, $\omega_n$ the corresponding theoretical value determined by means of the present model, and $N$ is the number of considered frequencies.

## 2.2 Identification based on forced displacements

In this study, harmonic forcing loadings are considered in addition to the self weight. Accordingly, it is not necessary to compare the time history of displacements but their maximum values corresponding to stationary vibrations. In this case, the objective function may be expressed as

$$FO = \sum_{m=1}^{M} \left( \frac{\tilde{v}_m - v_m}{\tilde{v}_m} \right)^2 \qquad (13)$$

where $\tilde{v}_m$ are the measured displacements, $v_m$ are the calculated ones and $M$ are the number of control points.

# 3 NUMERICAL MODEL

In order to solve the formulated problem, it is necessary to analyze different damage configurations given by the values adopted for $a_f$, $x_f$ and $l_f$, for which natural frequencies, for the problem 2.1, or forced displacements, for the problem 2.2, should be determined by means of equations (6-8). This task is performed by using FEM employing the FlexPDE software (2014). The calculation has two stages. Firstly, a sectional analysis has to be performed for the intact and the damaged cross-section, involving the solution of equation (2) and then the determination of the inertia and stiffness sectional coefficients given by expressions (9). These values are needed for solving the one-dimensional problem governed by the system (6-8).

Every analyzed scenery is evaluated according to the corresponding objective functions. The search of their minimum values is tackled by using an optimization technique known as Simulated Annealing. This last one is a stochastic method for searching the global minimum of a function and has the property to avoid staying trapped in a local minimum. Although the convergence is not assured, from the practical point of view, values very close to the optimum can be obtained.

The numerical model is implemented in the software Matlab (2010). From this last one FlexPDE (2014) is invoked.

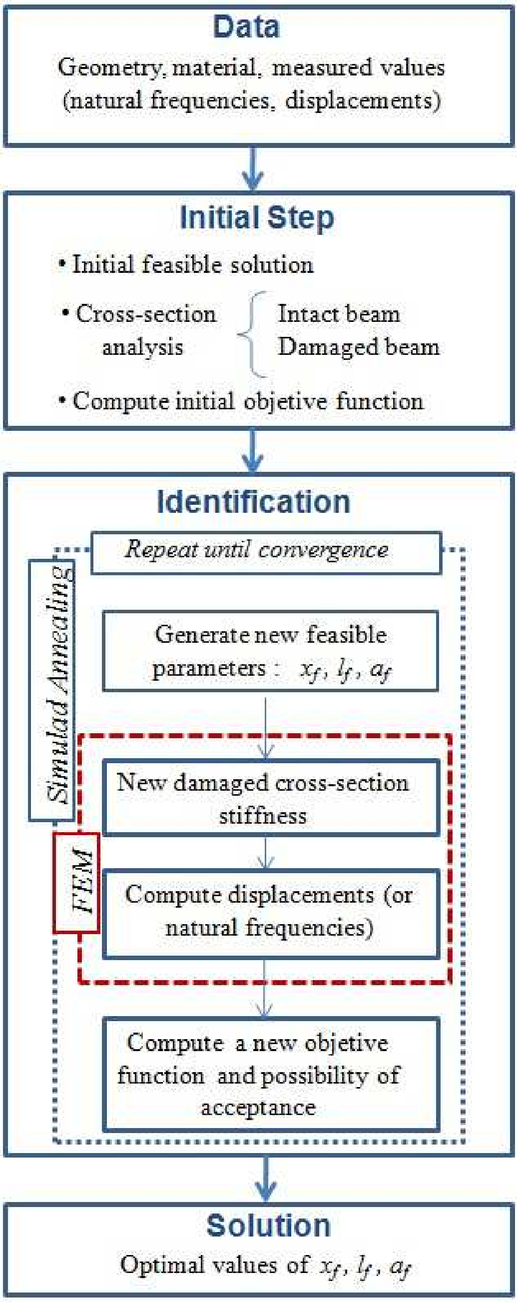


**Figure 3. Solution scheme**

# 4 NUMERICAL RESULTS

## 4.1 Validation of the proposed model

In order to validate the equations developed in section 1.1 and the corresponding numerical solution by means of FEM, two comparison studies are performed. In the first one, free vibrations of an intact asymmetric thin-walled beam made of aluminium are considered (see “Fig. 4”). Natural frequencies are calculated and compared with the corresponding values determined by Ambrosini & Danesi (2004). In the second place, free vibration of a damaged reinforced concrete beam (“Fig. 2”) is analyzed. The natural frequencies are determined by means of the present model and compared with those obtained by means of a 3-D finite element model.

The features of the aluminium beam shown in "Fig. 4" are the following: length $L = 2\,m$, density $\rho = 2650\,kg/m^3$, elasticity modulus $E = 4.5\text{x}10^{10}\,Pa$ and Poisson coefficient $\upsilon = 0.25$.

As shown in "Table 1", the natural frequencies obtained by the present approach have values very close to those determined by means of DYBEAM model by Ambrosini & Danesi with a mean difference of 2.4% approximately. These values compare with the experimental results in a more favourable form than those given by a finite element shell model (SAP2000).

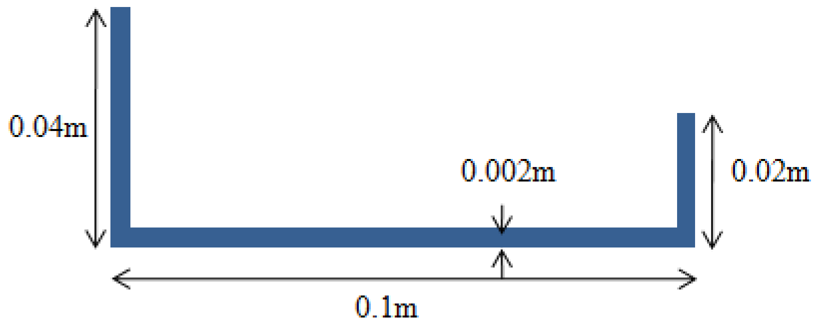


**Figure 4. Transverse section of the aluminium beam analyzed by Ambrosini & Danesi**

Table 1: Comparison of natural frequencies obtained by the present model and literature results

| | Clamped-clamped beam | | | | Clamped-free beam | | | |
|---|---|---|---|---|---|---|---|---|
| Frequency | Exp. | Present approach | DYBEAM | SAP2000 | Exp. | Present approach | DYBEAM | SAP2000 |
| $f_1$ | 24.5 | 24.2 | 24.8 | 22.2 | 5.2 | 5.2 | 5.3 | 5.15 |
| $f_2$ | 49.1 | 45.3 | 47.9 | 40.4 | 12.6 | 11.6 | 12 | 9.9 |
| $f_3$ | 63.5 | 61.3 | 63.4 | 55.2 | 25.8 | 23.3 | 23.4 | 22.4 |
| $f_4$ | ---- | 114.73 | ---- | ---- | 28.4 | 28.1 | 28.5 | 26.5 |
| $f_5$ | 122.5 | 121.03 | 119.1 | 102.8 | ---- | 48.5 | 50.9 | 41.9 |
| $f_6$ | ---- | 143.41 | ---- | ---- | 69.4 | 65.6 | 67.3 | 59.1 |

The second example analyzed corresponds to the reinforced concrete beam shown in "Fig. 2" whose dimensions and material characteristics are the following: length $L$=10 m, height $h$=0.5m, flange width $b_t$=1.8 m, web width $b$=0.15m, distance between webs $b_s$=0.9 m, flange thickness $e$=0.08 m, elasticity modulus $E$=3x10$^{10}$Pa, Poisson coefficient $\upsilon$=0.25

and density $\rho$ = 2400 kg/m$^3$. Damaged zone is identified by means of its length $l_f$, location with respect to the left end $x_f$ and depth of cracks $a_f$.

It should be observed that in order to determine the sectional rigidities, the effect of the reinforcement has been neglected. Certainly, this is not totally correct from the point of view of the accuracy of the model for representing the reality; however this simplification does not affect the validation under study. Of course, it is possible to consider the reinforcement effect by performing the determination of the sectional properties in a form slightly more complicated.

The first six natural frequencies for the hinged-hinged intact beam were determined and also the corresponding values for a damaged beam ($a_f$= 0.25 m, $l_f$= 4 m, $x_f$=2 m). The present results were compared with those calculated by means of a 3-D finite element model using FlexPDE software (2014). These values may be observed in "Table 2". As it is possible to appreciate, for both the damaged and the intact beam, the results given by the one-dimensional model are very similar to those calculated by the 3-D finite element method with a mean error of the order of 2%. Also, similar comparisons were performed in the case of forced vibrations, finding very small differences for the corresponding displacements.

Table 2: Comparison of natural frequencies obtained by the present model and a 3-D FEM

| Frequency | Intact | | Damaged | |
|---|---|---|---|---|
| | Beam | 3-D | Beam | 3-D |
| $f_1$ | 8.3 | 8.3 | 6.8 | 6.7 |
| $f_2$ | 14.9 | 15.1 | 15.3 | 15.6 |
| $f_3$ | 28.9 | 27.9 | 27.5 | 25.8 |
| $f_4$ | 33.0 | 32.3 | 29.2 | 27.8 |
| $f_5$ | 39.0 | 38.8 | 37.5 | 39.1 |
| $f_6$ | 72.9 | 72.7 | 64.6 | 62.5 |

## 4.2 Damage identification by means of natural frequencies

It is considered the same reinforced concrete beam analyzed in the last example, the section of which is shown in "Fig. 2". The effect of cracking on the first six natural frequencies is studied for both clamped and hinged ends. In "Table 3" the percentage differences between frequencies corresponding to intact and damaged beam may be observed.

For some modes, differences are sufficiently notable for being measured experimentally.

To carry out the identification, the first six values of natural frequencies are assumed to be known without measurement errors. Application of the present method yields optimum values for damage indicators as shown in the first rows of Tables "4" and "5" for clamped and hinged beams respectively.

Table 3.Comparison of natural frequencies corresponding to intact and damaged beams

| Frequency | Clamped-Clamped | | | Hinged-Hinged | | |
|---|---|---|---|---|---|---|
| | Intact | Damaged | % dif. | Intact | Damaged | % dif. |
| $f_1$ | 18.7 | 17.4 | 7.1 | 8.3 | 6.8 | 18.1 |
| $f_2$ | 21.8 | 22.2 | -1.9 | 14.9 | 15.3 | -2.7 |
| $f_3$ | 50.5 | 42.3 | 16.2 | 28.9 | 27.5 | 4.8 |
| $f_4$ | 52.3 | 52.0 | 0.6 | 33.0 | 29.2 | 11.5 |
| $f_5$ | 57.3 | 56.5 | 1.3 | 39.0 | 37.5 | 3.9 |
| $f_6$ | 94.0 | 75.6 | 19.7 | 72.9 | 64.6 | 11.4 |

In the following rows corresponding to the same tables, other damage parameters (obtained in other searches) are shown, yielding close values of the objective function. The corresponding errors have been defined in the following form:

$$Err_1 = \frac{a_f - \tilde{a}_f}{h} \quad Err_2 = \frac{x_f - \tilde{x}_f}{L} \quad Err_3 = \frac{l_f - \tilde{l}_f}{L} \tag{14}$$

where $\tilde{x}_f, \tilde{l}_f$ y $\tilde{a}_f$ correspond to the real parameters of the zone and $x_f, l_f, a_f$ are the values estimated using the model respectively.

Table 4. Damaged zone identified by means of natural frequencies: clamped-clamped beam

| Estimated damaged parameters (m) | | | Objective Function | Error (%) | | |
|---|---|---|---|---|---|---|
| $a_f$ | $x_f$ | $l_f$ | | *Err1* | *Err2* | *Err3* |
| 0.26 | 2.2 | 3.7 | 5.38E-05 | 2 | 2 | -3 |
| 0.28 | 2.3 | 3.3 | 2.34E-04 | 6 | 3 | -7 |
| 0.28 | 2.4 | 3.3 | 2.38E-04 | 6 | 4 | -7 |
| 0.26 | 2.0 | 3.7 | 4.16E-04 | 2 | 0 | -3 |

It is observed that error values are very small from the practical point of view for both end conditions.

Table 5. Damaged zone identified by means natural frequencies: hinged-hinged beam

| Estimated damaged parameters (m) | | | Objective Function | Error (%) | | |
|---|---|---|---|---|---|---|
| $a_f$ | $x_f$ | $l_f$ | | *Err1* | *Err2* | *Err3* |
| 0.24 | 2.0 | 4.1 | 2.01E-04 | -2 | 0 | 1 |
| 0.25 | 2.1 | 3.7 | 3.47E-04 | 0 | 1 | -3 |
| 0.28 | 2.2 | 3.3 | 5.54E-04 | 6 | 2 | -7 |
| 0.27 | 2.2 | 3.2 | 8.64E-04 | 4 | 2 | -8 |

It is interesting to note that if the search does not have reach the minimum value of the objective function, but close values as shown in rows 2 to 4 of Tables 4 and 5, the identified parameters values would even be acceptable, demonstrating the soundness of the methodology.

However, if the cracked zone is smaller, i.e. $a_f$ =0.25, $x_f$ =3 and $l_f = 0.5$, differences in frequency values would be scarcely notable (5.4% in the third frequency and lesser than 2% in the others). For this reason measurement errors would difficult the identification in a correct manner. This problem is due to the low sensivity of the frequencies with respect to small damages. This fact motivates the use of alternative indicators such as those analyzed in the next sub-section.

## 4.3 Identification using forced displacements

Forced displacements produced by a dynamic loading on a clamped-clamped beam whose section is shown in "Fig. 2" are analyzed. In particular two types of loading are considered. In the first case (Load 1), it is assumed a dynamic load $q_z = -1\text{x}10^4 \cos(\omega t)$ N/m applied on the first third of the length from the left end, over the right web (intact). Accordingly, this load produces a distributed torque given by $m_x = \text{-}0.45\text{x}10^4 \cos(\omega t)$ Nm/m. This dynamic loading is added to the self weight. The excitation frequency is $\omega = 0.8\omega_1$, being $\omega_1$ the fundamental frequency of the intact beam. Displacements measured at points corresponding to the inferior part of the web are analyzed.

In Figures "5" and "6" displacement values corresponding to Load 1 can be observed for different damage parameters. The damage effect is notable for the vertical displacements, especially when measured in the cracked web.

As second case the same loading is considered although applied to the damaged web (Load 2). For this case, differences of displacements with respect to the intact beam are even higher than those corresponding to Load 1. This fact may be appreciated in Figures "7" and "8".

For both loading states the damage kinematic effects are perfectly measurable.

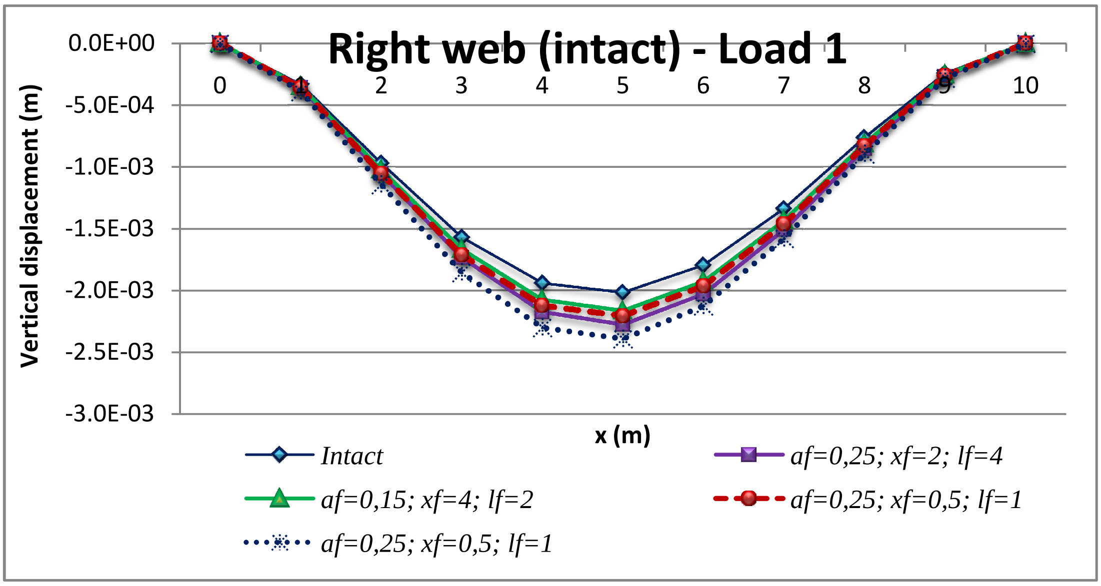


**Figure 5. Comparison of displacements corresponding to the intact web for Load 1 and different damage conditions**

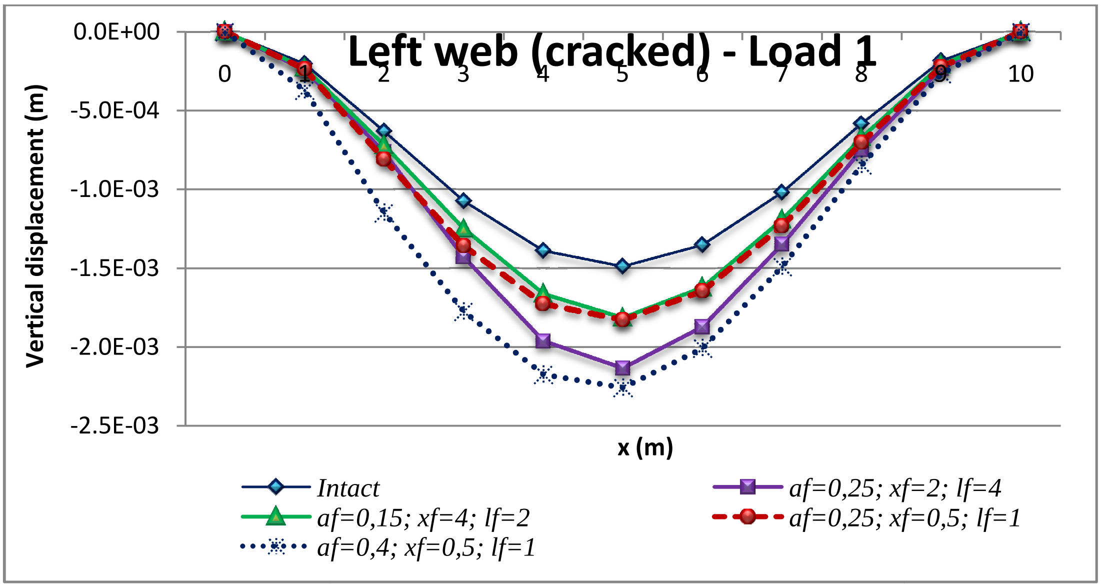


**Figure 6. Comparison of displacements corresponding to the damaged web for Load 1 and different damage conditions**

In order to analyze the identification problem, the following damage parameters are selected: $a_f = 0.25\text{m}, x_f = 2\text{m}$ and $l_f = 4\text{m}$. 18 locations (9 for each web) of the pseudo-experimental values are obtained by means of the theoretical model to which stochastic errors of ±5% are added, in order to represent model or measurement errors.

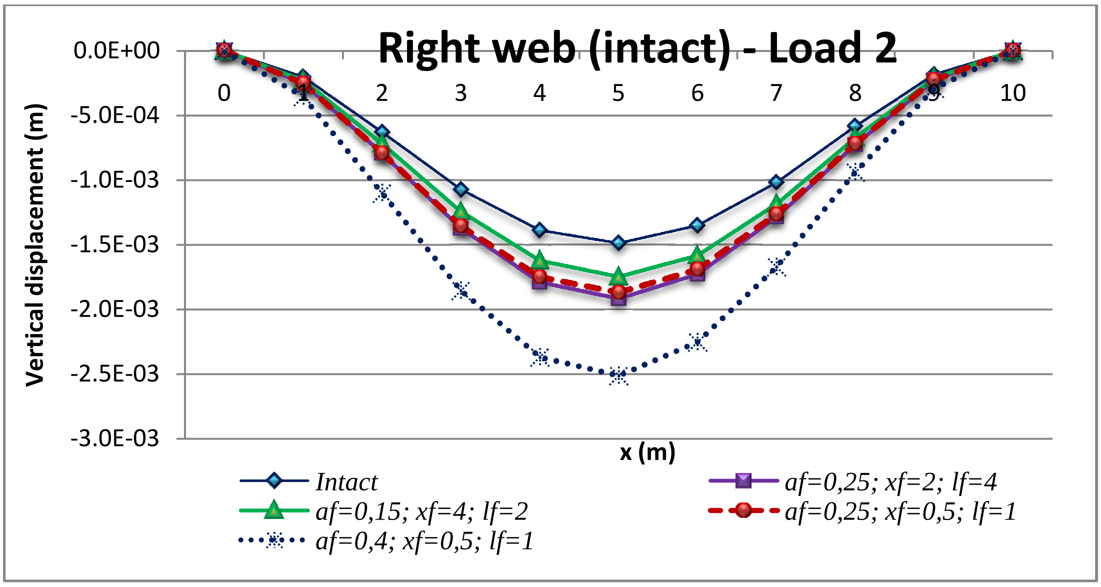


**Figure 7. Comparison of displacements corresponding to the intact web for Load 2 and different damage conditions**

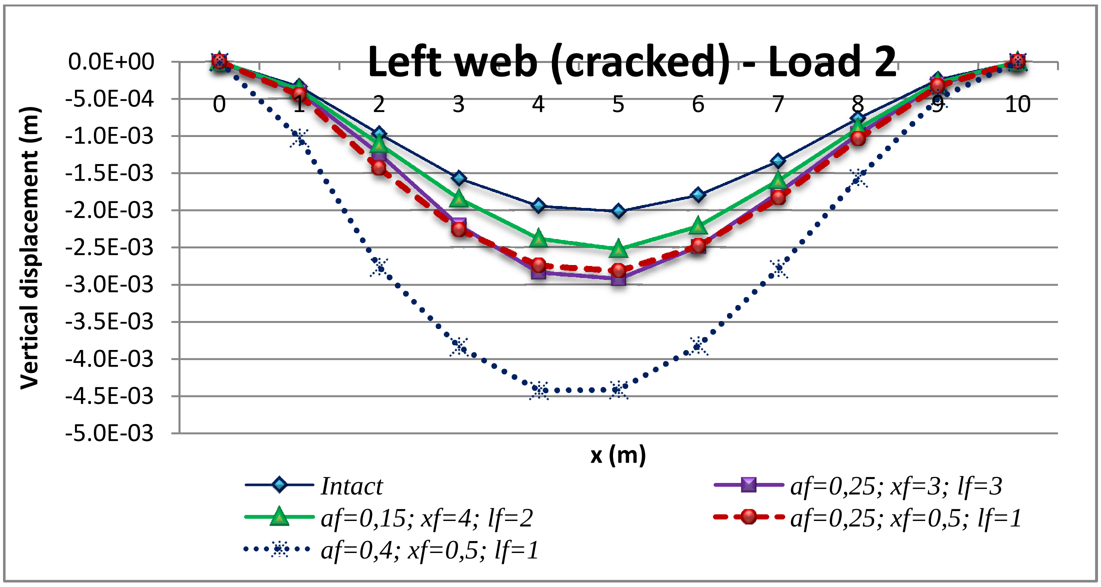


**Figure 8. Comparison of displacements corresponding to the damaged web for Load 2 and different damage conditions**

The identification is performed using three cases of loadings:

Case A: a concentrated load $P = -1\text{x}10^4 \cos(\omega t)\,\text{N}$ applied at the middle point of the length, over the right web (intact) of the beam.

Case B: the same load applied at a point distant 2 m from the left end, over the intact web.

Case C: the same load applied at a point distant 8 m from the left end, over the intact web.

With the corresponding data, the following cases of identifications have been performed:

Identification 1 (OF 1): data corresponding to Case A have been used.

Identification 2 (OF 2): data corresponding to Case B have been used.

Identification 3 (OF 3): data corresponding to Case C have been used.

Identification 4 (OF 4): data corresponding to Cases A, B and C in a simultaneous form have been used.

In the cases OF 1 and OF 4 the damaged zone has been determined in an exact form. In the cases OF 2 and OF 3, the procedure has failed in obtaining the exact solution. However, the determined values are very close to the exact ones.

On the other hand, the same calculation was carried-out using 8 points of measurements obtaining the same values for the damage parameters.

Table 5. Identification of damage zone parameters using different loads

| $a_f$ | $x_f$ | $l_f$ | OF 1 | OF 2 | OF 3 | OF 4 |
|---|---|---|---|---|---|---|
| 0.25 | 2.0 | 4.0 | 9.82E-03 | ---- | ---- | 2.98E-02 |
| 0.24 | 1.9 | 4.1 | ---- | ---- | 9.93E-03 | ---- |
| 0.24 | 1.9 | 4.0 | ---- | 9.92E-03 | ---- | ---- |

## CONCLUSIONS

A numerical procedure for identifying diffused cracking in thin-walled (thick-walled) beams was developed. The objective was to determine three parameters defining the damaged zone (location, length and depth) by minimizing the differences between calculated and measured values of magnitudes associated to the dynamic structural response (natural frequencies or displacements). The present procedure is based on a theoretical model for the three dimensional dynamics of non-homogeneous beams having arbitrary cross sectional shape.

The corresponding equations are solved by means of the Finite Element Method in order to evaluate the objective function and the Simulated Annealing technique is used to direct the search of damage parameters.

An extension of this research, considering non-linear properties of the involved materials (especially oriented to reinforced concrete), will be presented in the future.

## *Acknowledgements*

This work was supported by Secretaría de Ciencia y Tecnología de la Universidad Tecnológica Nacional, Departamento de Ingeniería de la Universidad Nacional del Sur and CONICET.

## REFERENCES

Ambrosini, D. & Danesi, R., (2004). Frecuencias naturales de vigas de pared delgada doblemente asimétricas. *Mecánica Computacional*, vol. 23, pp. 463-479.

Casas, J. & Aparicio A., (1994). Structural damage identification from dynamic-test data, *Journal of Structural Engineering*, vol. 120, n. 7, pp. 2437-2450.

Cerri, M. & Vestroni, F., (2000). Detection of damage in beams subjected to diffused cracking, *Journal of Sound and Vibration*, vol. 234, n. 2, pp. 259-276.

Cerri, M. & Vestroni, F., (2003). Use of frequency change for damage identification in reinforced concrete beams. *Journal of Vibration and Control*, vol. 9, pp.475-491.

Cortínez, V. & Dominguez, P., (2014). Identificación de fisuras por fatiga en vigas precargadas mediante el análisis dinámico no lineal. *Mecánica Computacional*, vol. 33, pp. 1487-1498.

Cortínez, V. & Dotti, F.; (2013). Mode I stress intensity factor for cracked thin-walled open beams. *Engineering Fracture Mechanics*, vol. 110, pp. 249-257.

Cortínez, V.; Dotti, F. & Reguera, F., (2014).Vibraciones no lineales de vigas de pared delgada precargadas, con fisura de fatiga. *Mecánica Computacional*, vol. 33, pp. 1499-1516.

Cortínez, V. & Piovan, M., (2002).Vibration and buckling of composite thin-walled beams with shear deformability, *Journal of Sound and Vibration*, vol. 258, n. 4, pp.701-723.

Dotti, F.; Cortínez, V. & Reguera, F., (2015).Non-linear dynamic response to simple harmonic excitation of a thin-walled beam with a breathing crack. *Appl. Math. Modelling.* doi:http://dx.doi.org/10.1016/j.apm.2015.04.052.

FlexPDE 6.36(2014).PDE Solutions Inc. www.pdesolutions.com

Hammed, E. & Frostig, Y., (2004). Free vibrations of cracked prestressed concrete beams. *Engineering structures*, vol. 26, pp. 1611-1621.

Matlab R2010a (2010).The MathWorks, Inc. www.mathworks.com.

Razak, H. & Choi, F., (2001). The effect of corrosion on the natural frequency and modal damping of reinforced concrete beams. *Engineering Structures*, vol. 23, pp. 1126-1133.

Zhu, X. & Law, S., (2007). A concrete-steel interface element damage detection of reinforced concrete structures. *Engineering structures*, vol. 29, pp.3515-3524.